Carbonate apatite increased osterix and BMP2 gene expressions and TNF-α and IL-6 reduced alkaline phosphatase activities via bone-related transcription factors in osteoblast-like cells

（炭酸アパタイトはオステリクスおよび骨形成タンパク質 2 遺伝子の発現を増加させ TNF-α および IL-6 は骨関連転写因子の発現を抑制し骨芽細胞様細胞でのアルカリホスファターゼ活性を減少させる）

日本大学大学院松戸歯学研究科歯学専攻

北澤　伊

（指導：小方　賴昌　教授）

Preface

This article is based on a main reference paper, “Carbonate apatite increases gene expression of osterix and bone morphogenetic protein 2 in the alveolar ridge after socket grafting’’ in the Journal of Oral Science, and a reference paper, “Suppression of Bone-related Transcription Factors by TNF-α and IL-6 Reduced Alkaline Phosphatase Activities in Osteoblast - like Saos2 Cells’’ in the International Journal of Oral-Medical Sciences.

Abstract

Alveolar ridge preservation by socket graft can attenuate bone resorption after tooth extraction. Runt-related transcription factor 2 (RUNX2), SP7/Osterix (OSX) and distal-less homeobox 5 (DLX5) are important transcription factors in osteoblast differentiation and bone formation. The purpose of this study was to evaluate effects of carbonate apatite (CO_3Ap) on osteoblast-related gene and protein expressions after socket graft, and to determine the effects of inflammatory cytokines on the expression of bone-related transcription factors and alkaline phosphatase (ALP) activities in human osteoblast-like Saos2 cells. Alveolar bone and new bone after CO_3Ap graft were collected at the time of implant placements. mRNA levels of RUNX2, SP7/OSX, bone morphogenetic protein 2

(BMP2), BMP7 and platelet derived growth factor B (PDGFB) were analyzed by real-time PCR. Immunostaining was performed using anti-RUNX2, SP7/OSX, vimentin and cytokeratin antibodies. To evaluate the bone resorption rates, cone-beam CT (CBCT) imaging was performed after socket graft and before implant placements. CBCT images showed that bone resorption rates at CO_3Ap graft sites was 7.15 ± 3.79%. In the graft sites, mRNA levels of SP7/OSX and BMP2 significantly increased. Replacement of CO_3Ap with osteoid was observed histologically, and osteoblast-like cells in the osteoid were stained by anti-SP7/OSX and vimentin antibodies.

Saos2 cells were stimulated by interleukin-1β (IL-1β; 1 ng/ml), tumor necrosis factor-α (TNF-α; 10 ng/ml) and interleukin-6 (IL-6; 10 ng/ml), and regulation of RUNX2, DLX5 and SP7/OSX mRNA and protein levels by IL-1β, TNF-α and IL-6 were analyzed by real-time PCR and Western blotting. Effects of IL-1β, TNF-α and IL-6 on alkaline phosphatase （ALP） mRNA levels and activities in Saos2 cells were confirmed by real-time PCR and ALP staining. IL-1β increased DLX5 mRNA and protein levels at 12 h. TNF-α suppressed RUNX2, DLX5 and SP7/OSX mRNA and protein levels at 12 and 24 h. IL-6 suppressed DLX5 and SP7/OSX mRNA and protein levels at 12 and 24. TNF-α and IL-6 suppressed ALP mRNA levels at 24 h, and ALP activities decreased after 3 days with TNF-α and IL-6.

Socket graft using CO_3Ap into the tooth extraction socket significantly increased SP7/OSX, BMP2 and vimentin expressions via BMP signaling pathway and promotes bone formation. TNF-α suppressed RUNX2, DLX5 and SP7/OSX expressions, and IL-6 inhibited DLX5 and SP7/OSX expressions and reduced ALP activities in Saos2 cells. From the above results, it is important that inflammatory responses, especially increases in inflammatory cytokines such as TNF-α and IL-6, do not occur during the bone formation process.

Introduction

Extraction sockets heal spontaneously without any intervention. However, when implants are placed in the alveolar ridge after tooth extraction, it is difficult to select the ideal position, implant diameter and length for the alveolar ridge where bone resorption has occurred. Araújo et al. observed morphological changes in the alveolar ridges in dogs 8 weeks after tooth extraction and reported that the height of buccal alveolar crest was 2 mm lower than the lingual bone crest (1). Chappuis et al. reported that the analyses using cone-beam computed tomography (CBCT), thickness of the human buccal bone after tooth extraction was average absorbed by 7.5 mm vertically, and 0.8mm horizontally at the anterior teeth (2). Implant placement becomes difficult if the alveolar ridge is

significantly lost after tooth extraction. Therefore, dental implants can only be placed after a socket graft or guided bone regeneration (GBR) is performed, and the grafted bone is stabilized. Alveolar ridge preservation by socket graft is performed to minimize morphological changes and volume loss due to alveolar bone resorption immediately after tooth extraction, and bone grafting materials are required (3). Recently, carbonated apatite (CO_3Ap) granules have been developed and used for maxillary sinus floor elevation and GBR to obtain the required bone height for placement of dental implants (4). Efficacy and safety of CO_3Ap granules for two-stage maxillary sinus floor elevation was evaluated by radiographic and histological methods using bone biopsies, and the results showed excellent biocompatibility and replaced to bone (5). When human bone marrow mesenchymal stem cells (hBMCs) cultured on hydroxyapatite (HA) or CO_3Ap discs, the growth rate of hBMCs were significantly faster than on cell culture dishes, and gene expressions of osteoblast differentiation markers such as alkaline phosphatase and osteocalcin were significantly increased (6). Maxillary sinus floor elevation was performed using HA, β-tricalcium phosphate (β-TCP) or deproteinized bovine bone mineral, and new bone tissues were collected from the graft sites at the time of implant placements to detect changes in gene expressions. Expression level of runt-related transcription factor 2 (RUNX2), key transcription factor associated with osteoblast

differentiation, was increased in deproteinized bovine bone mineral graft site compared to HA and β-TCP (7). Bone resorption 6 months after alveolar ridge graft using β-TCP or deproteinized bovine bone mineral has revealed that 17.5% of β-TCP and 1% of deproteinized bovine bone mineral were aborted (8). Therefore, there was a desire to develop an artificial bone with a low bone resorption rate, and CO_3Ap was born. Osterix (OSX, gene symbol: SP7) is another transcription factor downstream of RUNX2 that is essential for osteoblast differentiation (9). Bone morphogenetic protein 2 (BMP2) is a potent osteoinductive factor and has been widely reported to significantly promote osteogenic differentiation and new bone formation of mesenchymal stem cells (MSCs) (10). Platelet derived growth factor (PDGF) is a potent mitogen against a wide range of cell types, including fibroblasts, smooth muscle and bone marrow stromal cells (11). Vimentin is an intermediate filament characteristic of mesenchymal cells and a major cytoskeletal protein distributed in various cells such as fibroblasts, vascular endothelial cells, smooth and striated muscle cells, osteoblasts, chondrocytes, and nerve sheath cells which constitute connective tissues (12). Differences in the expression levels of osteoblast-related transcription factors, BMP2, PDGF and vimentin in newly generated alveolar bone harvested after CO_3Ap graft have not been reported.

Periodontitis is an inflammatory disease of the periodontal tissue caused by biofilm in

the periodontal pocket. If the causative agents in the periodontal pocket are not removed and the stimulations continue, excess amount of matrix metalloproteinase and inflammatory cytokines may induce connective tissue destruction and bone resorption (13). Inflammatory cytokines associated with periodontal disease include interleukin-1β (IL-1β), tumor necrosis factor-α (TNF-α) and interleukin-6 (IL-6), and the expressions were observed in gingival crevicular fluids of patients with periodontitis (14, 15). PDGF-BB and insulin-like growth factor-1 (IGF-1) suppressed cartilage degradation by IL-1β via down regulation of nuclear factor κB (NF-κB) (16). TNF-α inhibited osteocalcin (OC) expression in osteoblast-like cells (17). IL-6 suppressed collagen synthesis and alkaline phosphatase (ALP) activities in mouse osteoblast cell line (18). Transcription factors can bind to specific response elements in the gene promoter and stimulate or suppress the gene transcription (19). Moreover, RUNX2, SP7/OSX and distal-less homeobox 5 (DLX5) are important transcription factors for osteoblasts. RUNX2 is not expressed in fibroblasts and myoblasts, but highly expressed in osteoblasts. When undifferentiated mesenchymal stem cells were differentiated into osteoblasts with BMP7, RUNX2 and OC expressions were induced (20). In SP7/OSX null mice, expressions of early differentiation marker bone sialoprotein（BSP）was increased and late differentiation marker OC was suppressed, but RUNX2 expression did not change. On the other hand,

expression of SP7/OSX was suppressed in the RUNX2 knockout mice. The results suggest that RUNX2 is required for the expression of SP7/OSX (8). When osteoblasts isolated from murine calvaria from DLX5 null mice or wild-type mice were cultured in osteoblast differentiation medium, mRNA levels of RUNX2, SP7/OSX, BSP, OC and ALP were decreased in DLX5 null mic (21). Normal expression of RUNX2, SP7/OSX and DLX5 in osteoblasts may be important for maintaining bone homeostasis. Previously, there was no study to investigate the relationship between three kinds of inflammatory cytokines (IL-1β, TNF-α and IL-6) and bone-related transcription factors (RUNX2, SP7/OSX and DLX5) in osteoblast-like cells. The purpose of this study is to investigate the biochemical and histological evaluation of new bone obtained after CO_3Ap graft, and to evaluate the effects of inflammatory cytokines on mRNA and protein levels of osteoblast-related transcription factors and ALP.

Materials and Methods

Patient selection

There were 13 patients (7 males, and 6 females) for the alveolar bone harvesting control group, and 18 patients (6 males, and 12 females) for the CO_3Ap graft group were included in this study. Patients in the control group in this prospective study had already had

edentulous alveolar ridges at the time of their visit and requested implant treatments in those area. In the CO_3Ap graft group, patients had to extract their teeth due to fracture of teeth or severe periodontitis, and had CO_3Ap socket grafts at the time of tooth extraction and waited an average of 6.9 months to healing. Patients in the control group received initial periodontal therapy for an average of 6 months before starting implant treatments. The mean age of the patients was 58 years, ranging from 38 to 83 years (Table 3). This study was approved by the Institutional Internal Review and Ethics Board at the Nihon University School of Dentistry at Matsudo (EC20-25). All participants provided written informed consent. systemic and local exclusion criteria were defined as any factors interfering with dental implant surgery: severe liver, kidney, heart diseases, diabetes or poor oral hygiene.

CBCT measurements

To perform radiographic measurements, CBCT scans were taken after socket graft and at the implant placement (7 months after socket graft) for the measurements of vertical bone height and thickness of the buccal bone plate, and the results were processed using an open source software package (Slicer 3.6. www.slicer.org, National alliance for medical image computing, Boston, MA, USA). In order to calculate the bone resorption rates

(%),the vertical bone height from the alveolar bone crest to the bottom of extraction socket were compared after CO_3Ap graft and 7 months after socket graft (Fig. 1A).

Sample collections

During dental implant surgeries, alveolar bones were collected from the alveolar ridges and new bone after socket grafting with CO3Ap using trephine bar (Fig. 1B). Seven months after socket grafting with CO3Ap, new bone from graft sites were collected, and they were soaked in neutral formalin and stored at 4°C. The collected bone for RNA analyses were immersed in RNAlater™ (Thermo Fisher Scientific, Tokyo, Japan) and stored at -80°C.

Cell culture

Human osteoblast - like Saos2 cells（RCB0428）were purchased from RIKEN Cell Bank (Tokyo, Japan), and were cultured at 37°C in a 5% CO_2/95% air atmosphere in αMEM containing 10% fetal calf serum (FCS) and 1% penicillin and streptomycin. Saos2 cells (2×10^5/ml) were seeded in 60 mm tissue culture dishes, and were cultured 2 days until the cells were confluent. The culture media was then changed to αMEM without FCS for 12 h, and Saos2 cells were incubated in the no-serum αMEM with or without IL-1β (1

ng/ml), TNF-α (10 ng/ml) or IL-6 (10 ng/ml) for 12 and 24 h (22).

Real-time polymerase chain reaction (PCR)

Bone samples were pulverized and used immediately for total RNA isolation using a TRIzol RNA isolation reagents (Thermo Fisher Scientific). Total RNA was quantitated at 260 nm using a Nanodrop spectrophotometer (Thermo Fisher Scientific). cDNA was synthesized using PrimeScript RT reagent kit (Takara Bio, Tokyo, Japan). Quantitative real-time PCR for RUNX2, SP7/OSX, BMP2, BMP7, PDGF subunit B (PDGFB), DLX5 and ALP were carried out using TB Green Fast qPCR Mix in a TP950 thermal cycler dice real-time system (Takara Bio, Tokyo, Japan). The final reaction mixture (25 µl) containing TB Green Fast qPCR Mix (12.5 µl), 10 µM forward and reverse primers (final concentration, 0.2 µM), and 25 ng (2.0 µl) cDNA was used in the amplification reactions. Relative gene expression was calculated by the ΔΔCt method. The ΔΔCt was calculated using the reference gene GAPDH. The primers used in this study are presented in Table 1 and 2.

Immunohistochemistry

Alveolar bone and new bone after socket grafting with CO3Ap were collected and fixed

in 10% neutral buffered formalin and decalcification with 5% EDTA solution. Following the paraffin-embedded, 5 μm-thick sections were prepared. Bone tissue sections were stained using hematoxylin-eosin (H&E). Immunostaining for RUNX2, SP7/OSX, vimentin and cytokeratin in bone tissues were performed using the EnVisionTM + System, HRP (DAKO, Glostrup, Denmark). Bone tissue sections were manually dewaxed in 3 min xylene washes and rehydrated through incubation in graded ethanol to water. Endogenous peroxidase activity was destroyed by treating the sections with Histo VT One pH 7.0 for 20 min at 90°C. Sections were then washed three times in phosphate-buffered saline (PBS) for 5 min each. Following washing, sections were incubated in Protein Block Serum-Free (DAKO) for 10 min. Anti-RUNX2 (ab192256; Abcam, Cambridge, UK), SP7/OSX (ab22552; Abcam), vimentin (ab92547; Abcam) and cytokeratin (clone AE1, MAB1612; Merck, Darmstadt, Germany) antibodies were applied and tissue sections were incubated for overnight at 4°C. The sections were washed twice for 5 min with PBS before incubation with REAL EnVision-HRP, Rabbit-Mouse (DAKO) for 30 min at room temperature and treated with Substrate Working Solution (CHROM) for 3 min. sections were counterstained with Mayer's hematoxylin.

Western blotting

Radio immunoprecipitation (RIPA) Lysis Buffer Syste (sc-24948; Santa Cruz, Paso Robles, CA, USA) was used to Saos2 cells for total protein extraction. Total proteins were separated in 10% SDS-polyacrylamide gel electrophoresis and transferred onto polyvinylidene difluoride (PVDF) membrane. The membranes were incubated overnight at 4°C by anti-RUNX2 (ab23981; abcam), anti-DLX5 (ab64827; abcam), anti-SP7/Osterix (ab94744; abcam) and anti-actin (I-19; Santa Cruz Biotechnology) antibodies. To detection of the specific target protein, anti-rabbit IgG or anti-goat IgG conjugated with horse-radish peroxidase（Sigma - Aldrich Japan）was used as the secondary antibody. Immunoreactivities were detected by ELC plus Western blotting detection reagents. Image J software (National Institutes of Health, Bethesda, MD, USA) was used to quantify the band density.

ALP staining

ALP staining was performed on days 2 and 3 using Alkaline Phosphatase staining kit according to the manufacturer's protocol. On those days, the culture medium was removed, and the cell layers were rinsed with phosphate-buffered saline for 3 times and fixed in cold 10% neutral buffer formalin for 20 min at room temperature. After 20 min, the cell layers were washed with purified water. Then, the fixed cells were incubated with

buffer containing substrate - containing buffer and chromogenic substrate. After 20min at 37°C, the cell layers were washed with purified water and observed grossly.

Statistical Analysis

Patients data are shown as mean ± standard deviation (SD) in Table 3 and 4. The significance of differences between alveolar bone and new bone after socket grafting with CO3Ap for bone-related transcription factors and growth factor mRNA expression levels were determined by the Steel-Dwass test and presented as the median and interquartile range. The level of significance was adjusted at 5%. Statcel: the useful addin forms on Excel, 4th ed. (OMS Ltd. Publisher, Tokyo, Japan) was used for statistical analyses (23). Triplicate samples were analyzed for each experiment, and experiments were replicated to ensure the consistency of the response to IL-1β, TNF-α and IL-6. Significance of difference between the control and IL-1β, TNF-α or IL-6 was determined using one-way ANOVA and Tukey-Kramer test.

Results

Participants were divided into two groups: alveolar bone harvesting control group and CO_3Ap graft group in the extraction socket. There were 13 patients (7 males, and 6

females) in the alveolar bone harvesting control group, with a mean age of 58.4 ± 12.5 years. In the CO_3Ap graft group, there were 18 patients (6 males, and 12 females) with a mean age of 60.7 ± 17.8 years (Table 3). The average healing period after socket graft was 6.9 ± 2.7 months, and bone resorption rate after socket graft was 7.15 ± 3.79% (Table 3). Implant placement sites where bone harvested are shown in the lower part of Table 3. Vertical bone height and thickness of the buccal bone plate after CO_3Ap graft and vertical bone height 7 months after socket graft in the CO_3Ap graft group were shown in Table 4. There was no correlation between thickness of the buccal bone plate and bone resorption rate. Effects of CO_3Ap socket graft on the expressions of osteoblast-related genes is yet unknown. In the CO_3Ap graft group, mRNA levels of SP7/OSX and BMP2 were significantly increased compared with the alveolar bone harvesting control group (Fig. 2A, C). However, expression levels of RUNX2, PDGFB and BMP7 mRNA were not increased significantly (Fig. 2A, C, 3A). There was no difference in RUNX2, SP7/OSX, BMP2, PDGFB and BMP7 mRNA expressions between the maxillary and mandibular bone graft sites (Fig. 2B, D, 3B). Osteoid matrix formation was seen 7 months after the socket graft with CO_3Ap, suggesting that the CO_3Ap accelerated calcification in the area of new bone formation (Fig. 4A, B, C). Immunohistochemical analyses were performed on the tissue sections of the new bone after socket grafting with CO_3Ap. The cells around

the osteoid were more strongly stained by anti-SP7/OSX and anti-vimentin antibodies (Fig. 4G, H, I, J, K, L) than anti-RUNX2 antibody (Fig. 4D, E, F). Cytokeratin, an epithelial marker, was not detected in the cells around the osteoid (Fig. 4M, N, O).

The mRNA levels of RUNX2, DLX5, SP7/OSX and osteogenic marker ALP were analyzed in osteoblast-like Saos2 cells stimulated by IL-1β（1 ng/ml）, TNF-α（10 ng/ml） or IL-6 (10 ng/ml). RUNX2 mRNA levels were significantly suppressed by TNF-α at 12 and 24 h. DLX5 and SP7/OSX mRNA levels were significantly reduced by TNF-α and IL-6 at 12 and 24 h. ALP mRNA levels were significantly inhibited by TNF-α and IL-6 at 24 h. However, IL-1β did not change the mRNA levels of RUNX2, SP7/OSX and ALP, and significantly increased DLX5 mRNA level (Fig. 5A, B, C). To determine the effects of IL-1β, TNF-α or IL-6 on RUNX2, DLX5 and OSX protein levels, Saos2 cells were stimulated with IL-1β (1 ng/ml), TNF-α (10 ng/ml) or IL-6 (10 ng/ml). IL-1β significantly increased DLX5 protein levels at 12 and 24 h, but did not change RUNX2 and OSX protein levels (Fig. 6A). TNF-α significantly decreased RUNX2, DLX5 and OSX protein levels at 12 and 24 h (Fig. 6B). IL-6 significantly decreased DLX5 and OSX protein levels at 24 h, and at 12 and 24 h (Fig. 6C). To examine the effects of IL-1β, TNF-α and IL-6 on ALP activities in osteoblasts, ALP staining was performed 2 and 3 days after stimulation. ALP staining of Saos2 cells were inhibited 3 days after TNF-α and IL-6 stimulations (Fig.

7).

Discussion

In this study, we have shown that CO_3Ap increased SP7/OSX and BMP2 gene expressions in alveolar ridges after socket grafting. Compared to autologous bone graft, artificial bone grafts have disadvantage that they do not fit well with the existing bone and take long time to healing. However, they have advantage of not being invasive to the patient. Typical synthetic graft materials used for artificial bone graft are HA, β-TCP and CO_3Ap. After transplantation, β-TCP reacts with body fluids, degrades, absorbs and replaces it with surrounding new bone. Solubility of β-TCP in the body fluids is higher than that of HA (24). Comparative study using CBCT for alveolar bone resorption 6 months after alveolar ridge graft using β-TCP or deproteinized bovine bone mineral has revealed that 17.5% of β-TCP and 1% of deproteinized bovine bone mineral were aborted. Bone resorption after socket graft was smaller when deproteinized bovine bone mineral was used (8). In this study, an average of 7.15% bone resorption was observed about 7 months after CO_3Ap graft, indicating that CO_3Ap causes less bone resorption than β-TCP (Table 1). RUNX2 and SP7/OSX are osteoblast-related transcription factors and have been reported to be involved in osteoblast differentiation and bone formation (9, 20).

SP7/OSX mRNA levels were significantly increased in new bone 7 months after CO_3Ap grafting (Fig. 2). Although RUNX2 expression is observed in SP7/OSX knockout mice, SP7/OSX expression is not detected in RUNX2 knockout mice (9). The result suggests that the SP7/OSX is downstream gene of RUNX2. On the other hand, BMP2 induced SP7/OSX transcription through Dlx5 independently of RUNX2 (25). BMP2 induced the osteogenic differentiation of MSCs, and stimulates SP7/OSX expression via Dlx5 transcription factor (25, 26). PDGF-BB promotes bone regeneration by enhancing the osteogenic and angiogenic abilities of bone marrow stromal cells (10). Gene therapy using PDGFB avoided osteomalacia and increased trabecular bone formation in mice through increased expressions of SP7/OSX and RUNX2 (27). In this study, mRNA level of BMP2 was increased significantly in new alveolar bone after socket graft with CO_3Ap (Fig. 2). Ridge augmentation is performed when the alveolar bone width and height are insufficient to place the dental implant in the proper position, and decortication is applied in combination with bone graft (28-31). Histological views of H&E staining showed that the osteoid formation was observed at the site of CO_3Ap graft (Fig. 4A, B, C). Similar to the previous studies, CO_3Ap granules exhibited excellent biocompatibility, and bone biopsies demonstrated that they could replace human bone (5). SP7/OSX and BMP2 mRNA levels were increased significantly by CO_3Ap graft, and H&E staining of the bone

tissues revealed that CO_3Ap was replaced by osteoid. This study suggests that differentiation of osteoblasts is induced at the site of CO_3Ap graft, unlike existing bone. Furthermore, results of immunostaining suggest that SP7/OSX could induce osteoblast differentiation mediated through the BMP pathway after CO_3Ap grafting.

In the second study, it has shown that the suppression of bone-related transcription factors by TNF-α and IL-6 reduced ALP activities in osteoblast-like Saos2 cells. Destruction of periodontium is evoked by overproduction of inflammatory cytokines, reduction of osteoblast activities, and activation of osteoclasts (12). In this study, we have shown that the inflammatory cytokines associated with periodontitis might regulate expressions of bone-related transcription factors in osteoblast-like Saos2 cells. IL-1β increased DLX5 mRNA and protein levels at 12 and 24 h. TNF-α suppressed RUNX2, DLX5 and SP7/OSX mRNA and protein levels. IL-6 suppressed DLX5 and SP7/OSX mRNA and protein levels (Fig. 5 and 6). IL-1β significantly increased expression of BMP2 in human periodontal ligament stem cells (hPDLSCs) and activated NF-κB, mitogen-activated protein kinase and Smad signaling pathways (32). BMP-2 increased SP7/OSX expression is mediated through DLX5, but independent of RUNX2 (26). Lipopolysaccharide（LPS）inhibited embryonic bone mineralization via activating NF-κB and stimulating the TNF-α and IL-6 releases. TNF-α and IL-6 caused the induction of

retinoic acid synthetase-cytochrome P450 1B1 expression and subsequently activated retinoic acid signaling, that may inhibit DLX5 transcription directly, and restricted bone formation (33). IL-6 and soluble receptor of IL-6 significantly inhibited ALP activity, and gene expressions of RUNX2, SP7/OSX and OC (34). Following treatment of hPDLSCs with TNF-α, ALP and RUNX2 mRNA levels were significantly decreased compared with the control untreated hPDLSCs (35). The antineoplastic drug etoposide suppressed the protein expressions of RUNX2 and OSX in osteoblasts and reduced the intensity of ALP staining (36). In this study, we showed that the treatments of Saos2 cells with TNF-α suppressed RUNX2, DLX5, SP7/OSX and ALP gene expressions (Fig. 1B). TNF-α decreased RUNX2, DLX5 and SP7/OSX, and IL-6 inhibited DLX5 and SP7/OSX protein expressions (Fig. 6B, C). In addition, the intensity of ALP staining decreased after 3 days with TNF-α and IL-6 treatments (Fig. 7). These suggest that RUNX2, DLX5 and SP7/OSX may play crucial role for osteoblast differentiation. RUNX2 mRNA and protein expressions were suppressed only by TNF-α treatment (Fig. 5B and 6B). In nocodazole-treated MC3T3-E1 cells, RUNX2 mRNA level was elevated, but protein level was decreased, indicating RUNX2 mRNA levels are increased at mitosis in osteoblasts (37). Therefore, the presence of RUNX2 may be important for maintaining the characteristics of osteoblasts. TNF induces RUNX2 degradation mediated through up-regulations of

Smurf1 and Smurf2 in osteoblasts (38). Moreover, suppression of RUNX2 by TNF-α decreased osteogenic differentiation and inhibited bone formation in MC3T3-E1 osteoblast-like cells (39). IL-1β inhibited osteogenic potential of periodontal ligament stem cells (PDLSCs), however low dose of IL-1β promoted the osteogenesis of PDLSCs. Therefore, IL-1β might increase mRNA levels of DLX5 at low concentrations. IL-6 inhibited mRNA and protein levels of DLX5 and SP7/OSX, but did not inhibit RUNX2. TNF-α was thought to be most involved in alveolar bone resorption due to periodontitis and to inhibit osteoblast maintenance and bone formation by suppressing bone-related transcription factors RUNX2, DLX5 and SP7/OSX.

Reference

1. Araújo MG, Lindhe J. Dimentional ridge alterations following tooth extraction. An experimental study in the dog. J Clin periodontal, 32: 212-218, 2005.
2. Chappuis V, Engel O, Shahim K, Reyes M, Katsaros C, Buser D. Soft tissue alterations in esthetic postextraction sites: A 3-dementional analysis. J Dent Res, 94: 187S-193S, 2015.
3. Iasella JM, GreenWell H, Miller RL, Hill M, Drisko Scheetz JP. Ridge preservation with freeze-dried bone allograft and a collagen membrane compared to extraction

alone for implant site development: clinical and histologic study in humans. J Periodontol, 74: 990-999, 2003.

4. Kudoh K, Fukuda N, Kasugai S, Tachikawa N, Koyano K, Matsushita Y, Ogino Y, Ishikawa K, Miyamoto Y. Maxillary Sinus Floor Augmentation Using low-crystalline carbonate apatite granules with simultaneous implant installation: First-in-human clinical trial. J Oral Maxillofac Surg, 77: 985.e1-985.e11, 2019.
5. Nakagawa T, Kudoh K, Fukuda N, Kasugai S, Tachikawa N, Koyano K, Matsushita Y, Sasaki M, Ishikawa K, Miyamoto Y. Application of low-crystalline carbonate apatite granules in 2-stage sinus floor augumentation: a prospective clinical trial and histomorphometric evaluation. J Periodontal and Implant Science, 49: 382-396, 2019.
6. Nagai H, Kobayashi-Fujioka M, Fujisawa K, Ohe G, Takamaru N, Hara K, Uchida D, Tamatani T, Ishikawa K, Miyamoto Y. Effects of low crystalline carbonate apatite on proliferation and osteoblastic differentiation of human bone marrow cells. J Mater Sci Mater Med 26: 99, 2015.
7. Caubet J, Ramis JM, Ramos-Murguialday M, Morey M Á, Monjo M. Gene expression and morphometric parameters of human bone biopsies after maxillary sinus floor elevation with autologous bone combined with Bio-Oss® or BoneCeramic®. Clin Oral Implants Res, 26: 727-735, 2015.

8. Jung RE, Philipp A, Annen BM, Signorelli L, Thoma DS, Ha¨mmerle CHF, Attin T, Schmidlin P. Radiographic evaluation of different techniques for ridge preservation after tooth extraction: a randomized controlled clinical trial. J Clin Periodontol, 40: 90-98, 2013.
9. Nakashima K, Zhou X, Kunkel G, Zhang Z, Deng JM, Behringer RR, Crombrugghe BD. The novel zinc finger-containing transcription factor osterix is required for osteoblast differentiation and bone formation. Cell, 108: 17-29, 2002.
10. Shen H, Zhuang Y, Zhang C, Zhang C, Yuan Y, Yu H, Si J, Shen G. Osteoclast- Driven Osteogenesis, Bone Remodeling and Biomaterial Resorption: A New Profile of BMP2-CPC-Induced Alveolar Bone Regeneration. Int J Mol Sci, 23: 12204, 2022.
11. Zhang M, Yu W, Niibe K, Zhang W, Egusa H, Tang T, Jiang X. The effects of platelet-derived growth factor-BB on bone marrow stromal cell-mediated vascularized bone regeneration. Stem Cells International, 3272098, 2018.
12. Franke WW, Schmid E, Osborn M, Weber K (1979) Intermediate-sized filaments of human endothelial cells. J Cell Biol. 81, 570-580.
13. Page RC, Kornman KS: The pathogenesis of human periodontitis: an introduction. Periodontol 2000, 14: 9 - 11, 1997.
14. Yavuzyilmaz E, Yamalik N, Bulut S, Özen S, Ersoy F, Saatpi Ü: The gingival

crevicular fluid Interleukin-1β and tumor necrosis factor-α levels in patients with rapidly progressive periodontitis. Aust Dent J, 40: 46 - 49, 1995.

15. Kurti Biilent, Develioglu H, Taner ÏL, Balo K, Tekin ÏÖ: IL - 6 levels in gingival crevicular fluid（GCF）from patients with non - insulin dependent diabetes mellitus（NIDDM）, adult periodontitis and healthy subjects. J Oral Sci, 41: 163 - 167, 1999.
16. Montaseri A, Busch F, Mobasheri A, Buhrmann C, Aldinger C, Rad JS, Shakibaei M: IGF - 1 and PDGF-bb suppress IL-1β - induced cartilage degradation through down-regulation of NF-κB signaling: Involvement of Src/PI - 3K/AKT pathway. PLoS One, 6: e28663, 2011.
17. Gilbert L, He X, Farmer P, Boden S, Kozlowski M, Rubin J, Nanes MS: Inhibition of osteoblast differentiation by tumor necrosis factor-alpha. Endocrinology, 141: 3956 - 3964, 2000.
18. Ishimi Y, Miyaura C, Jin CH, Akatsu T, Abe E, Nakamura Y, Yamaguchi A, Yoshiki S, Matsuda T, Hirano T: IL-6 is produced by osteoblasts and induces bone resorption. J Immunol, 145: 3297 - 3303, 1990.
19. Latchman DS: Transcription factors: an overview. Int J Biochem Cell Biol, 29: 1305 - 1312, 1997.
20. Ducy P, Zhang R, Geoffroy V, Ridall AL, Karsenty G. Osf2/Cbfa1: a transcriptional

activator of osteoblast differentiation. Cell, 89: 747-754, 1997.

21. Samee N, Geoffroy V, Marty C, Schiltz C, Vieux-Ro-chas M, Levi G, de Vernejoul MC: DLX5, a positive regulator of osteoblastogenesis, is essential for osteoblast - osteoclast coupling. Am J Pathol, 173: 773 - 780, 2008.
22. Blaschke M, Koepp R, Cortis J, Komrakova M, Schieker M, Hempel U, Siggelkow H: IL - 6, IL - 1β, and TNF-α only in combination influence the osteoporotic phenotype in Crohn's patients via bone formation and bone resorption. Adv Clin Exp Med, 27: 45 - 56, 2018.
23. Hisae Yanai. (2015) Statcel : the useful addin forms on Excel, 4th ed. OMS Ltd. Publisher.
24. Neo M, Nakamura T, Ohtsuki C, Kokubo, Yamamuro T. Apatite formation on three kinds of bioactive material at an early stage in vivo: a comparative study by transmission electron microscopy. J Biomed Mater Res, 27: 999-1006, 1993.
25. Lee MH, Kwon TG, Park HS, Wozney JM, Ryoo HM. BMP-2-induced osterix expression is mediated by Dlx5 but is independent of Runx2. Biochem Biophys Res Commun, 309: 689-694, 2003.
26. Cai H, Zou J, Wang W, Yang A. BMP2 induces hMSC osteogenesis and matrix remodeling. Mol Med Rep, 23: 125, 2021.

27. Chen W, Baylink DJ, Jones JB, Neises A, Kiroyan JB, Rundle CH, Lau KHW, Zhang XB, PDGFB-based stem cell gene therapy increases bone strength in the mouse. Proc Natl Acad Sci USA, 112: 3893-3900, 2015.

28. Hämmerle CH, Karring T. Guided bone regeneration at oral implant sites.Periodontol 2000, 17: 151-175, 1998.

29. Canto FRT, Garcia SB, Issa JPM, Marin A, Bel EAD, Defino HLA. Influence of decortication of the recipient graft bed on graft integration and tissue neoformation in the graft-recipient bed interface. Eur Spine J, 17: 706–714, 2008.

30. Lee SH, Lim P, Yoon HJ. The influence of cortical perforation on guided bone regeneration using synthetic bone substitutes: a study of rabbit cranial defects. Int J Oral Maxillofac Implants, 29: 464-471, 2014.

31. Acar AH, Yolcu U. Bone decortication rate and guided bone regeneration under an occlusive titanium dome: Micro-CT analysis. Annals of Medical Research, 26: 329-334, 2019.

32. Mao CY, Wang YG, Zhang X, Zheng XY, Tang TT, Lu EY: Double-edged -sword effect of IL - 1β on the osteogenesis of periodontal ligament stem cells via crosstalk between the NF-κB, MAPK and BMP/ Smad signaling pathways. Cell Death Dis, 7: e2296, 2016.

33. You L, Zhu L, Li PZ, Wang G, Cai H, Song J, Long D, Berman Z, Lin L, Cheng X, Yang X: Dysbacteriosis - derived lipopolysaccharide causes embryonic osteopenia through retinoic - acid - regulated DLX5 expression. Int J Mol Sci, 21: 2518, 2020.

34. Kaneshiro S, Ebina K, Shi K, Higuchi C, Hirao M, Okamoto M, Koizumi K, Morimoto T, Yoshikawa H, Hashimoto J: IL - 6 negatively regulates osteoblast differentiation through the SHP2/MEK2 and SHP2/ Akt2 pathways in vitro. J. Bone Miner. Metab, 32: 378 – 392, 2014.

35. Yuan J, Wang X, Ma D, Gao H, Zheng D, Zhang J: Resveratrol rescues TNF-α-induced inhibition of osteogenesis in human periodontal ligament stem cells via the ERK1/2 pathway. Mol Med Rep, 21: 2085–2094, 2020.

36. Nakashima H, Yasunaga M, Yoshida M, Yamaguchi M, Takahashi S, Kajiya H, Tamaoki S, Ohno J: Low concentration of etoposide induces enhanced osteogenesis in MG63 cells via Pin1 activation. J Hard Tissue Biol, 30: 175-182, 2021.

37. Galindo M, Pratap J, Young DW, Hovhannisyan H, Im HJ, Choi JY, Lian JB, Stein JL, Stein GS, van Wijnen AJ: The bone-specific expression of RUNX2 oscillates during the cell cycle to support a G1-related antiproliferative function in osteoblasts. J Biol Chem, 280: 20274 – 20285, 2005.

38. Kaneki H, Guo R, Chen D, Yao Z, Schwarz EM, Zhang YE, Boyce BF, Xing L: Tumor

necrosis factor promotes RUNX2 degradation through up-regulation of Smurf1 and Smurf2 in osteoblasts. J Biol Chem, 281: 4326 - 4333, 2006.

39. Gilbert L, He X, Farmer P, Rubin J, Drissi H, van Wijnen AJ, Lian JB, Stein GS, Nanes MS: Expression of the osteoblast differentiation factor RUNX2 （Cbfa1/ AML3/Pebp2alpha A）is inhibited by tumor necrosis factor - alpha. J Biol Chem, 277: 2695 - 2701, 2002.

Table 1 Primers used for real-time PCR analysis (Study1)

Gene symbol	Primers
GAPDH	Fwd: GCACCGTCAAGGCTGAGAAC
	Rev: ATGGTGGTGAAGACGCCAGT
RUNX2	Fwd: ATGTGTTTGTTTCAGCAGCA
	Rev: TCCCTAAAGTCACTCGGTATGTGTA
SP7/OSX	Fwd: GCCATTCTGGGTTGGGTATC
	Rev: GAAGCCGGAGTGCAGGTATCA
BMP2	Fwd: ATGGATTCGTGGTGGAAGTG
	Rev: GTGGAGTTCAGATGATCAGC
PDGFB	Fwd: GATACTTTGCGCGCACACAC
	Rev: GGTTTTCTCTTTGCAGCGAGG
BMP7	Fwd: TGGCAGCATCCAATGAACAAGATCC
	Rev: TTCCTTTCGCACAGACACCAATGTG

Table 2 Primers used for real-time PCR analysis (Study2)

Gene symbol	Primers
GAPDH	Fwd: GCACCGTCAAGGCTGAGAAC
	Rev: ATGGTGGTGAAGACGCCAGT
RUNX2	Fwd: ATGTGTTTGTTTCAGCAGCA
	Rev: TCCCTAAAGTCACTCGGTATGTGTA
DLX5	Fwd: AGCTACGCTAGCTCCCTACCACC
	Rev: GGTTTGCCATTCACCATTCTCAC
OSX	Fwd: GCCATTCTGGGTTGGGTATC
	Rev: GAAGCCGGAGTGCAGGTATCA
ALP	Fwd: GGACCATTCCCACGTCTTCAC
	Rev: CCTTGTAGCCAGGCCCATTG

Table 3 Patient characteristics of the alveolar bone harvesting control group and CO_3Ap graft group

	Control group	CO_3Ap graft group
Males	**7**	**6**
Females	**6**	**12**
Total	**13**	**18**
Age	**58.4 ± 12.5**	**60.7 ± 17.8**
Healing period after socket grafting (month)		**6.9 ± 2.7**
Bone resorption rate (%)		**7.15 ± 3.79**

Implant placement sites where bone harvested	Alveolar bone	CO_3Ap graft sites
Maxillary anteriors	**0**	**0**
Maxillary premolars	**1**	**5**
Maxillary molars	**1**	**5**
Mandibular anteriors	**0**	**0**
Mandibular premolars	**3**	**2**
Mandibular molars	**8**	**6**

Carbonate apatite (CO_3Ap). Error bars indicate the ± SD (n = 13: Alveolar bone, n = 18: CO_3Ap graft)

Table 4 Vertical bone height and thickness of the buccal bone plate after CO_3Ap graft and vertical bone height 7 months after socket graft in CO_3Ap graft group

No. of Patients	Vertical bone height just after socket graft	Vertical bone height when implant placement	Bone resorption rate (%)	Thickness of the buccal bone plate just after socket graft
1	12.0	11.6	3.33	1.1
2	11.3	10.5	7.08	0.7
3	10.0	9.1	9.00	3.5
4	11.1	10.3	7.21	1.6
5	11.8	11.5	2.54	1.1
6	10.8	10.2	5.56	0.9
7	13.6	12.5	8.09	1.0
8	10.2	9.4	7.84	0.5
9	11.3	10.4	7.96	1.6
10	11.9	11.1	6.72	2.1
11	8.1	7.6	6.17	2.9
12	9.3	8.5	8.60	0.7
13	10.1	9.1	9.90	0.8
14	9.9	9.8	1.01	1.6
15	10.5	10.1	3.81	1.3
16	9.6	9.2	4.17	0.9
17	8.6	7.1	17.4	0.7
18	11.4	10.0	12.3	1.3
Mean ± SD	10.6 ± 1.3	9.9 ± 1.4	7.15 ± 3.79	1.35 ± 0.79

Carbonate apatite (CO_3Ap)

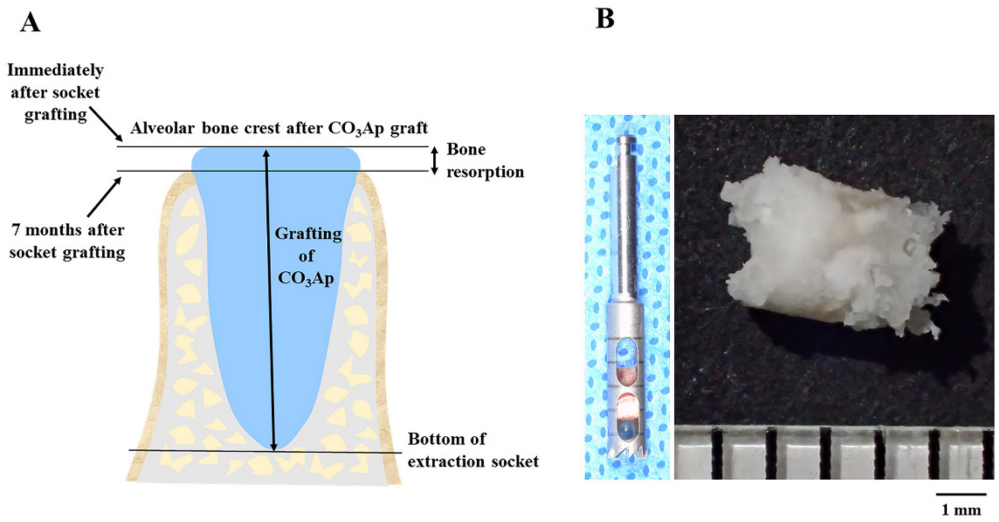

Fig. 1 Schematic diagram for calculation of bone resorption rate and photograph of harvested bone and trephine bar. (A) CBCT slice section of CO_3Ap graft site at baseline. To calculate the bone resorption rates, alveolar bone crests after CO_3Ap graft and 7 months after socket graft were compared. Bone resorption rates (%) = bone resorption / bottom of extraction socket from alveolar bone crest after CO_3AP graft × 100. (B) Left panel; Trephine bar used for bone harvesting. Right panel; Pictures of harvested bone 7 months after CO_3Ap graft. Bottom scale is 1 mm.

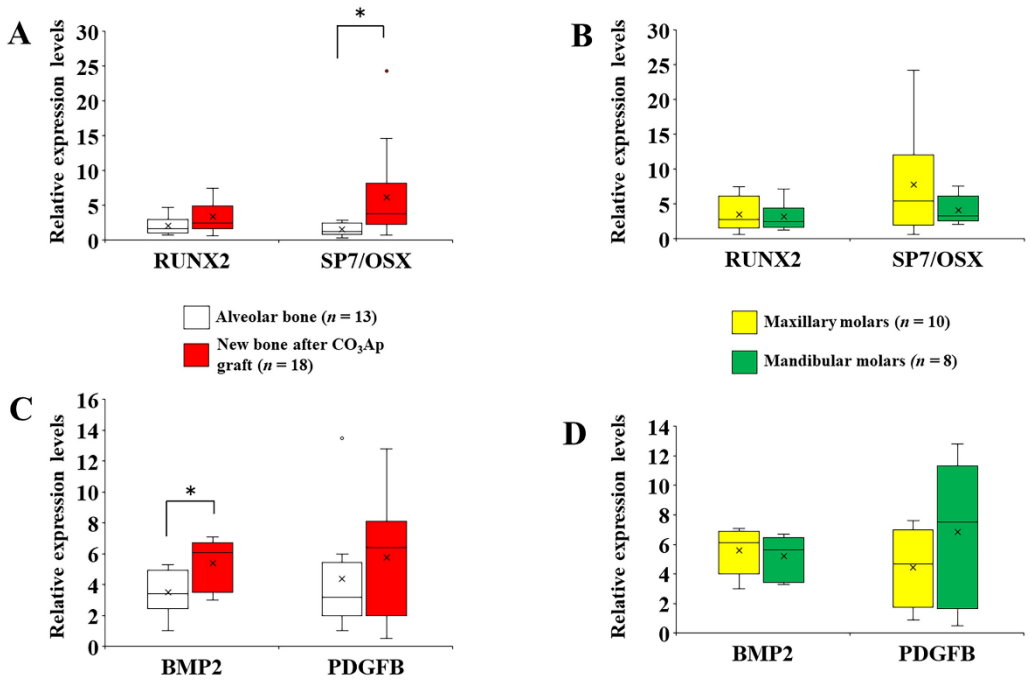

Fig. 2 Relative expression levels of RUNX2, SP7/OSX, BMP2 and PDGFB. (A) mRNA levels of RUNX2 and SP7/OSX in the alveolar bone (n = 13) and CO_3Ap graft sites (n = 18) were shown by box plots (Median and Interquartile range). (B) mRNA levels of RUNX2 and SP7/OSX in the maxillary molars (n = 10) and mandibular molars (n = 8) after socket graft with CO_3Ap were shown by box plots. (C) mRNA levels of BMP2 and PDGFB in the alveolar bone and CO_3Ap graft sites were shown by box plots. (D) mRNA levels of BMP2 and PDGFB in the maxillary molars and mandibular molars after socket graft with CO_3Ap were shown by box plots. *$P < 0.05$.

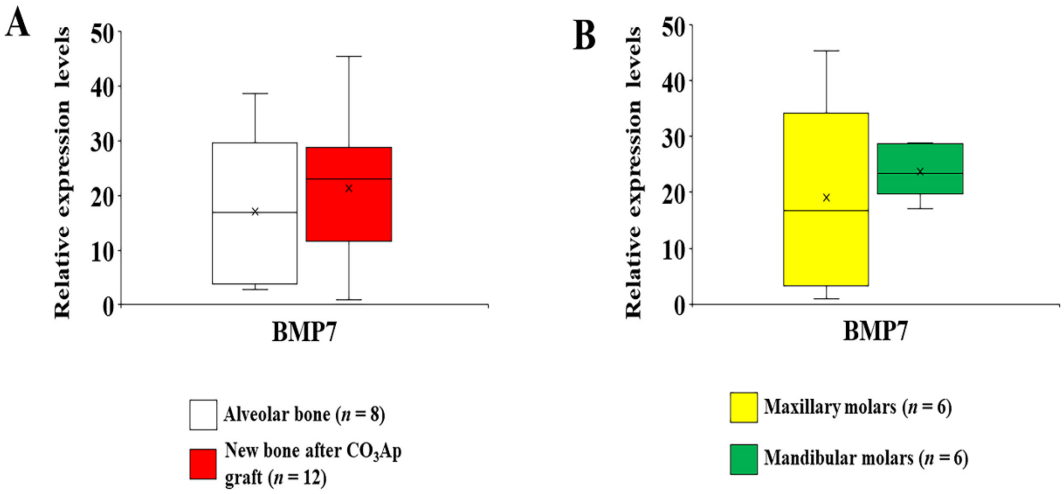

Fig. 3 Relative expression levels of BMP7. (A) mRNA levels of BMP7 in the alveolar bone (n = 8) and CO_3Ap graft sites (n = 12) were shown by box plots (Median and Interquartile range). (B) mRNA levels of BMP7 in the maxillary molars (n = 6) and mandibular molars (n = 6) after socket graft with CO_3Ap were shown by box plots.

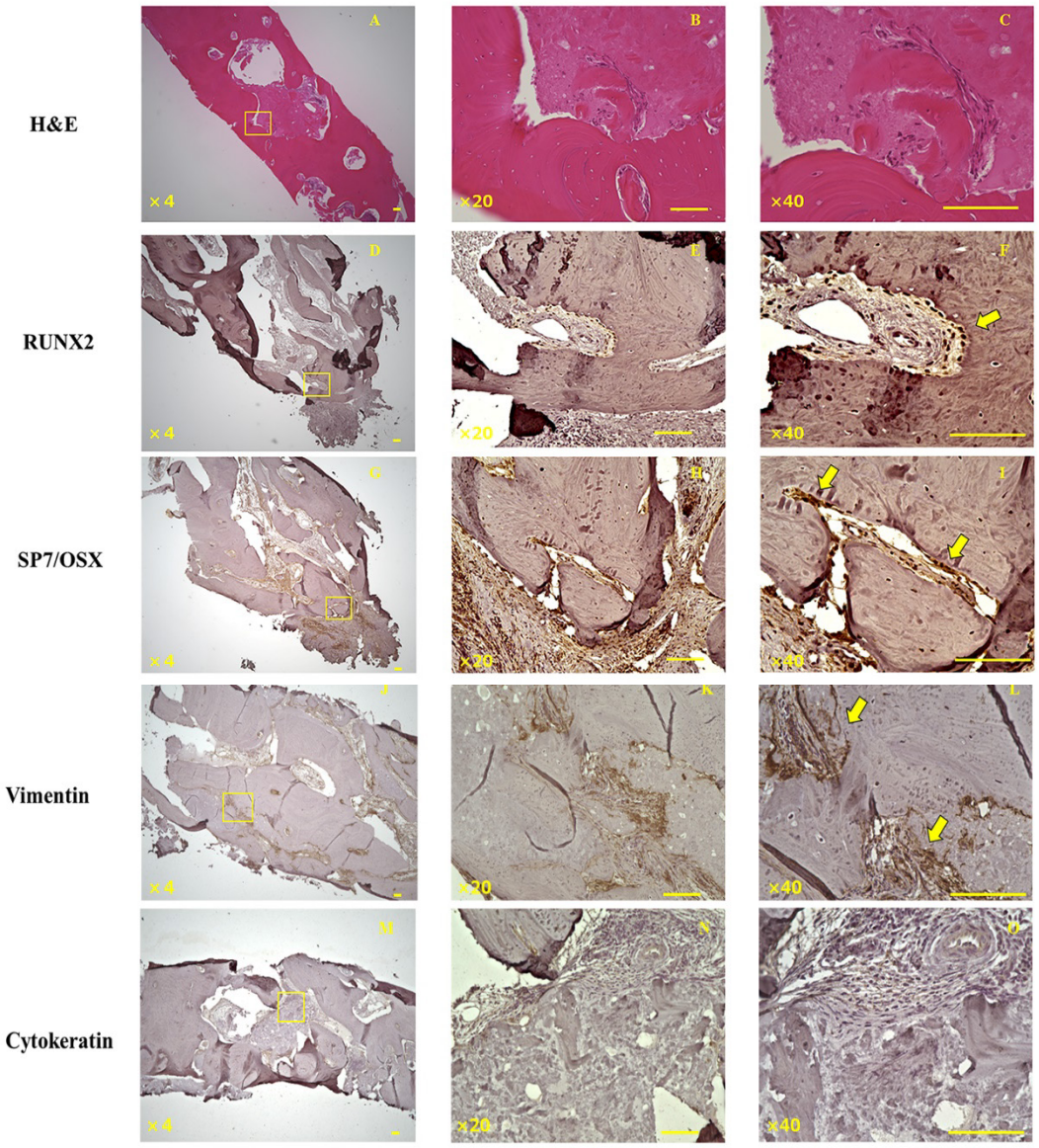

Fig. 4 Histological and immunohistochemical analyses of bone tissue after CO_3Ap socket grafting. (A, B, C) H&E stain of bone biopsies. Immunohistochemical analyses of bone biopsies: (D, E, F) RUNX2, (G, H, I) SP7/OSX, (J, K, L) Vimentin and (M, N, O) Cytokeratin. Osteoid formations were observed at the sites of CO_3Ap graft (A; ×4, B; ×20, C; ×40). (D, E, F) RUNX2, (G, H, I) SP7/OSX and (J, K, L) vimentin-positive cells were observed around the osteoid (arrow). Yellow bars represent 100 μm, respectively.

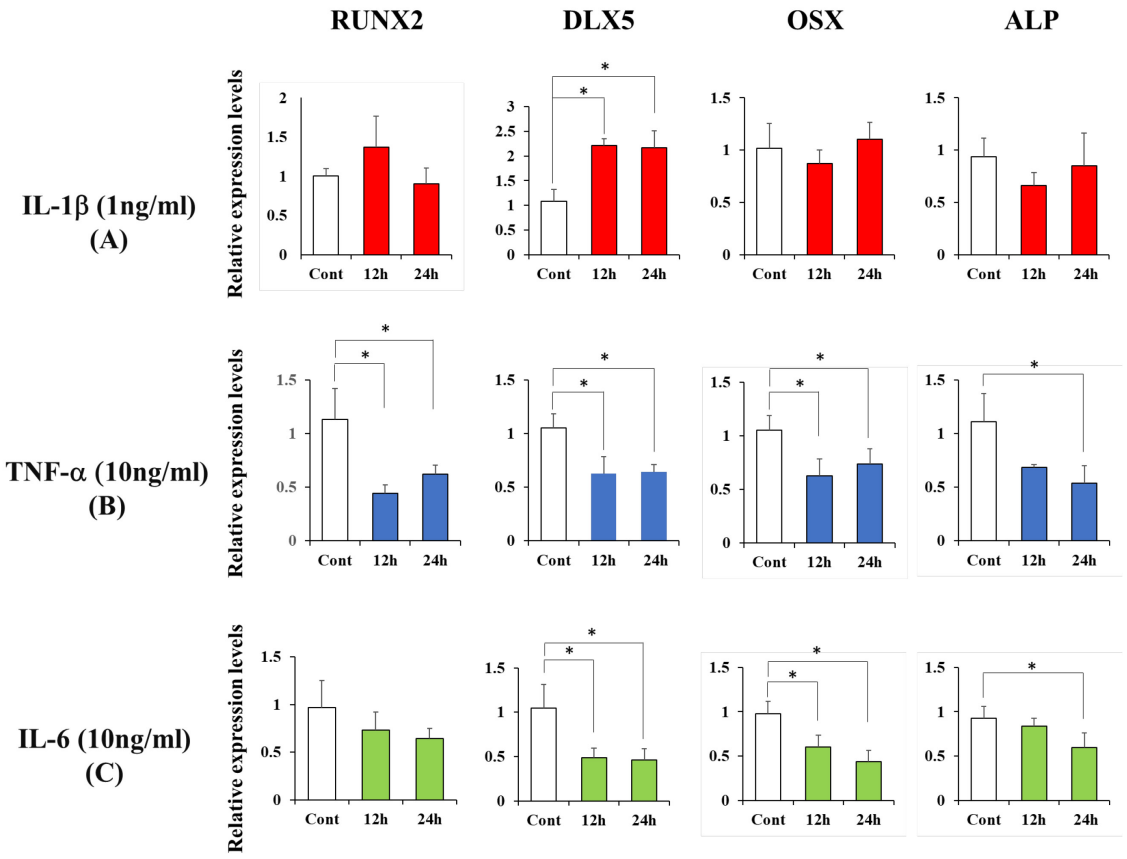

Fig. 5 Effects of IL-1β, TNF-α and IL-6 on the mRNA levels of RUNX2, DLX5, OSX and osteogenic marker ALP in the osteoblast-like Saos2 cells. Saos2 cells were treated with IL-1β (A), TNF-α (B) and IL-6 (C). Total RNAs were extracted, and the mRNA expressions of RUNX2, DLX5, OSX and ALP were analyzed by real-time PCR.

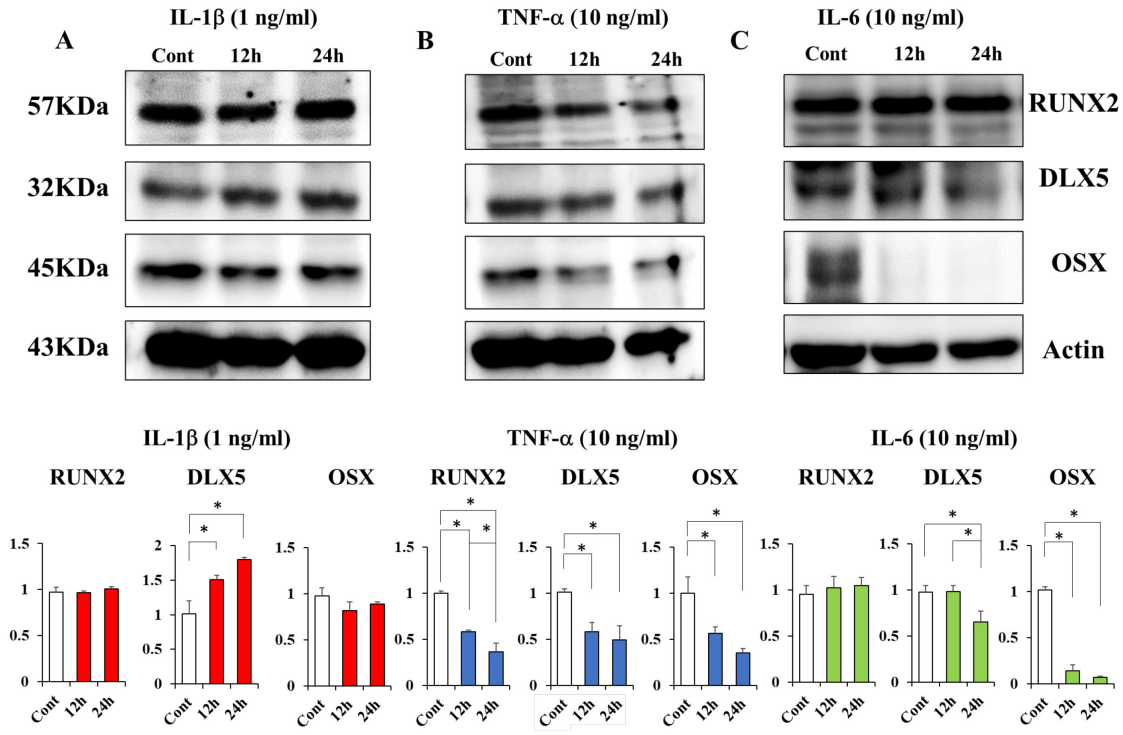

Fig. 6 Osteoblast-like Saos2 cells were stimulated by IL-1β (A), TNF-α (B) and IL-6 (C). Total proteins were extracted, and the protein expressions of RUNX2, DLX5, OSX and Actin were analyzed by Western blotting. Densitometric quantifications of the results of Western blot for RUNX2, DLX5 and OSX. Data represent mean ± SD from three experiments (P<0.05) differences between control and experimental groups (IL-1β, TNF-α and IL-6).

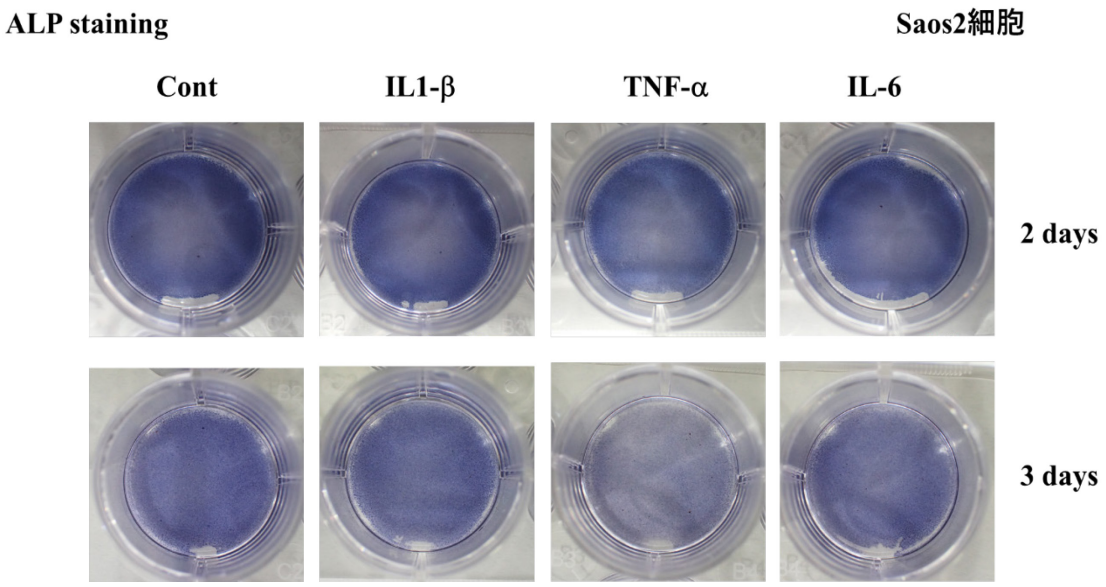

Fig. 7 Effects of IL-1β, TNF-α and IL-6 on ALP activities in Saos2 cells. Saos2 cells were treated with IL-1β (1 ng/ml), TNF-α (10 ng/ml) or IL-6 (10 ng/ml) for 2 and 3 days.